An Improved Minor Loop Gain Criterion and Stability Estimation for Multi-Inverters Paralleled System

Yuhan DUAN, Pingjuan GE, Hailiang XU, and Hongbin LIN

***Abstract*—With the increasing popularity of new energy integration, the parallel operation of multiple inverters in power systems has become commonplace. Traditional theories and methods for analyzing power system stability face challenges in high-proportion new energy systems. Additionally, existing inverter analysis methods are inadequate for directly addressing multi-inverters paralleled system, resulting in unclear instability mechanisms and uncertain operational stability. To tackle these issues, this paper focuses on systems with multiple parallel LCL-type inverters and proposes an improved minor loop gain criterion (IMLG). Unlike traditional impedance ratio criteria, this improved criterion fully integrates considerations such as inverter capacity, short-circuit ratio, and other pertinent factors affecting system stability. Furthermore, treating each inverter as a subsystem by equivalent the grid conductance to the inverter side, this criterion accurately identifies the primary inverter responsible for system instability. Finally, case and experimental studies are employed to verify the correctness of the theoretical analysis and demonstrate the effectiveness of the improved stability criterion.**

***Index Terms*—Admittance modeling, multi-inverters paralleled system, minor loop gain criterion, responsibility for instability.**

I. Introduction

CONFRONTING the increasingly severe energy crisis and the continuously growing demand for electricity, new energy generation systems have attracted significant attention [1], [2]. With the continuous increase in the proportion of new energy devices, the strength of the power systems gradually get weakened, exhibiting weak grid characteristics [3], which in turn raises the risk of instability issues.

Grid-connected inverters, as the interface unit between power generation and the grid, play a crucial role in electrical energy conversion [4], [5]. However, when numerous inverters are interconnected with the grid, harmonic interactions between them can pose significant stability risks, potentially threaten system safety [6]−[8]. This issue becomes especially critical under weak grid conditions, where dynamic interactions among multiple grid-connected inverters can lead to broad-spectrum resonance problems. Moreover, the varied grid connection environments, circuit topologies, and control strategies employed by grid-connected inverters complicate the study of resonance issues in multi-inverters system [9]−[11].

Currently, there are two primary methods for modeling and analyzing stability issues in grid-connected inverter systems. One method utilizes a transfer function impedance model in the frequency domain, while the other involves developing a state-space model in the time domain [12]−[14]. The impedance models for grid-connected inverters include the *dq* impedance model based on synchronous rotating coordinate transformation and the sequence impedance model based on harmonic linearization [15]−[17]. Building upon the impedance model, the impedance analysis is applied to analyze stability in grid-connected inverter systems [18]. The impedance analysis method was initially used for stability analysis in DC-DC systems [19], and later adapted and applied to assess stability in AC systems [20]−[22]. Compared to the state-space method, impedance analysis avoids the computation of high-order system state matrices by splitting the system into two subsystems and employs the Nyquist criterion for stability analysis, providing distinct advantages.

In recent years, researchers have conducted extensive studies on the stability issues of multi-inverters grid-connected system. These studies focus on utilizing impedance analysis principles for stability assessment in grid-connected inverters. Typically, stability analysis in inverter grid-connected systems employs impedance ratio formulations. The criterion in [23] is extended to multi-inverters grid-connected system, treating each inverter as a subsystem, while regarding the other inverters and the grid as a separate subsystem. The stability is determined by satisfying the Nyquist criterion based on the admittance ratio between these two subsystems. In contrast, in [24], it alters the system's equivalent form by examining the ratio between the total output admittances of all grid-connected inverters and the admittances of other grid components for analysis. However,

Manuscript received June 28, 2024; revised September 12, 2024; accepted October 8, 2024. Date of publication December 30, 2024; date of current version October 21, 2024. This work was supported by the National Natural Science Foundation of China under the grant 52077222 and 52307230, and the Shandong Provincial Natural Science Foundation under the grant ZR2023QE156. *(Corresponding author: Pingjuan Ge.)*

Y. Duan, P. Ge, and H. Xu are with the College of New Energy, China University of Petroleum (East China), Qingdao 266580, China (e-mail: z23150039@s.upc.edu.cn; gepingjuan@upc.edu.cn; xuhl@upc.edu.cn).

H. Lin is with the College of New Energy, China University of Petroleum (East China), Qingdao 266580, China, and also with the Shanghai Jiao Tong University, Shanghai 200240, China (e-mail: Linhongbin@s.upc.edu.cn).

Digital Object Identifier 10.24295/CPSSTPEA.2024.00023

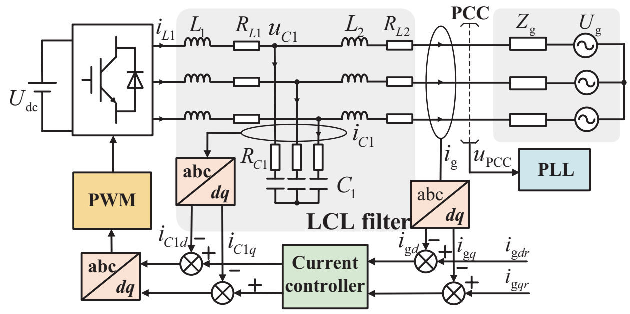

Fig. 1. LCL-type grid-connected inverter structure.

this approach treats all inverters collectively and lacks specificity in analyzing the stability of individual inverters. In [25], the grid line impedance is considered as part of the inverters' grid-side inductance, exploring the open-loop transfer function of the system. Nevertheless, this method is not suitable for multi-inverters paralleled system with varying parameters.

In conclusion, an improved impedance analysis criterion is urgently needed to study the stability of multi-inverters paralleled system and to accurately analyze the stability of multi-inverters paralleled system. Therefore, based on the small-signal admittance model of grid-connected inverters and impedance analysis principles, this paper introduces an improved stability analysis criterion that incorporates the rated capacity of each inverter. This enhanced criterion allows for precise evaluation of each inverter's operational condition and accurate identification of the particular inverter contributing to instability. Finally, through analysis of experimental results, the validity of the theoretical analysis and the effectiveness of the refined criterion were confirmed.

II. Improved Minor Loop Gain Stability Criterion

In this section, based on impedance analysis, an improved minor loop gain criterion (IMLG) that can indirectly reflect the short-circuit impedance ratio of the inverter equipment is proposed by equating the grid conductance to the inverter's line conductance and considering the inverter's rated capacity. The proposed criterion effectively assesses the stability of grid-connected inverters and precisely identifies which inverters are responsible for instability. This approach enables accurate stability analysis of multi-inverters grid-connected system.

A. The Conventional Loop Gain Stability Criterion

In view of the benefits of LCL-type filters, such as excellent filtering performance, wide application and mature research, this paper selects LCL-type grid-connected inverters as the research object [26]−[28].

Fig. 1 depicts the configuration of an LCL-type grid-connected inverter, which includes the inverter-side inductance L_1, the filter capacitor C_1, the grid-side inductance L_2 and its parasitic resistance R_{L1}, R_{C1}, R_{L2}. The grid impedance is Z_g. In the figure, U_{dc}, u_{PCC} stand for the DC-side voltage and grid connection point voltage, respectively; u_{C1}, U_g are the filter capacitor voltage grid voltage, while i_{C1}, i_g are the corresponding current.

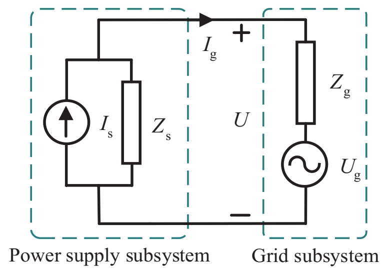

Fig. 2. Equivalent circuit model of a grid-connected inverter.

The current loop adopts PI controller, and its transfer function expression is as follows:

$$G_i = k_{pi} + \frac{k_{ii}}{s} \tag{1}$$

where k_{pi}, k_{ii} are the proportional and integral coefficients, respectively.

The impedance analysis method usually divides the grid-connected system into two subsystems, source-side and grid-side, and the equivalent circuit model of the grid-connected inverter system is shown in Fig. 2. The power supply subsystem consists of a current source I_s in parallel with the equivalent impedance Z_s, while the grid side consists of a voltage source U_g in series with the grid impedance Z_g. In this paper, the calculation of the inverter output impedance is based on the actual values.

Based on Fig. 2, the grid-connected current can be expressed as:

$$I_g(s) = \left[I_s(s) - \frac{U_g(s)}{Z_s(s)}\right] \cdot \frac{1}{1 + Z_g(s)/Z_s(s)} \tag{2}$$

Referring to (2), it can be seen that the stability of a single inverter grid-connected system depends on whether the ratio of the grid impedance to the output impedance of the grid-connected inverter satisfies the Nyquist criterion, i.e., $Z_g(s)/Z_s(s)$. If the value of $Z_g(s)/Z_s(s)$ satisfies the Nyquist criterion, i.e., the Nyquist curve does not encircle the point $(-1, j0)$, the system is in stabilization.

For the multi-inverters paralleled system, the stability criteria commonly used in the impedance analysis method are also based on the impedance ratio. These mainly include the minor loop gain (MLG) and the global minor loop gain (GMLG) [23], [24].

The MLG is defined as the ratio between the output admittance of a certain inverter and the total admittances observed from the inverter's port, as illustrated in Fig. 3. And the inverter is equivalent to a current source, paralleled with its output admittance Y_{si}, where i denotes the i-th inverter. The grid is modeled as an ideal voltage source U_g, in series with the output admittance Y_g. The grid current i_g represents the combined output currents of the inverters, denoted by i_{si}. Therefore, the expression for MLG can be formulated as:

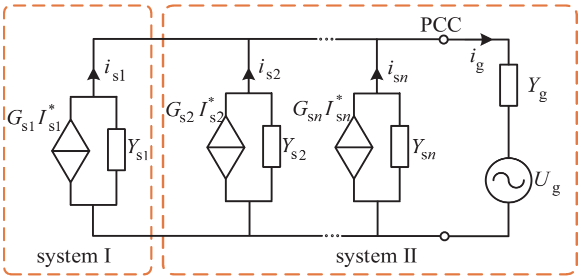

Fig. 3. Equivalent circuit diagram for MLG.

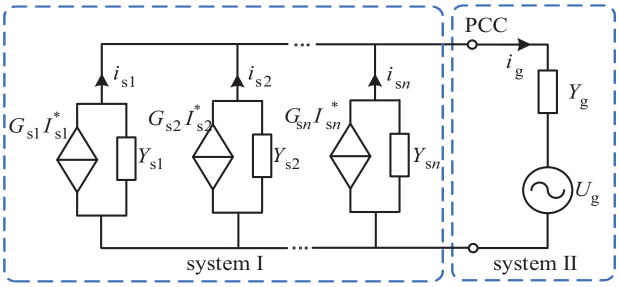

Fig. 4. Equivalent circuit diagram for GMLG.

$$MLG_i = Y_{si} / \left(Y_g + \sum_{j=1,\, j\neq i}^{n} Y_{sj} \right) \tag{3}$$

where j represents inverters other than i, and n is the total number of inverters in the grid-connected system. It is important to note that in Fig. 3, the first inverter is designated as a subsystem (i.e., $i = 1$) in the MLG expression, while the remaining inverters and the grid constitute another subsystem. Consequently, the grid-connected current for the i-th inverter can be derived as:

$$I_{si} = \frac{G_{si} I_{si}^{*}}{1+MLG_i} - \frac{1}{1+\left(1/MLG_i\right)} \bullet \left(\sum_{j=1,\, j\neq i}^{n} G_{sj} I_{sj}^{*} + U_g Y_g \right) \tag{4}$$

The GMLG represents the ratio of the total output admittances of all grid-connected inverters to the combined admittances of the grid and passive components. Essentially, it treats all inverters collectively as one subsystem and considers the grid admittance along with the admittance of passive components as another subsystem, analyzing the interactions between these two subsystems. This setup is depicted in Fig. 4, and the expressions are provided as follows:

$$GMLG = \left(\sum_{i=1}^{n} Y_{si} / Y_g \right) = Z_g \sum_{i=1}^{n} Y_{si} \tag{5}$$

Since the GMLG criterion considers all inverters collectively, the grid-connected current for the inverter can be expressed as:

$$I_g = \frac{1}{1+GMLG} \sum_{i=1}^{n} \left(G_{si} I_{si}^{*} - U_g Y_{si} \right) \tag{6}$$

In an ideal grid, the stability of inverters is inherently ensured during the design phase, meaning G_{si} and Y_{si} do not possess poles in the right-half-plane. Similarly, Y_g, as a passive element with inherent damping, also lacks right-half-plane poles [29].

Conventional methods require MLG_i to meet Nyquist stability criteria to ensure system stability. Referring to (4) , it can be seen that in order to make the system stable, $1/MLG_i$ should also satisfy the Nyquist stability criterion. Therefore, without incorporating the analysis of $1/MLG_i$, the MLG criterion alone cannot accurately perform stability analysis for parallel system. However, conducting a synergistic analysis using both MLG_i and $1/MLG_i$ would add complexity to the stability analysis of multi-inverters grid-connected system. Moreover, since the GMLG criterion treats all grid-connected inverters as a single subsystem, it only provides an overview of the system's stability and cannot individually assess the operation of each inverter.

Therefore, there is an urgent need for an improved minor loop gain criterion that can accurately attribute instability to specific inverters when conducting stability analyses of multi-inverters grid-connected system.

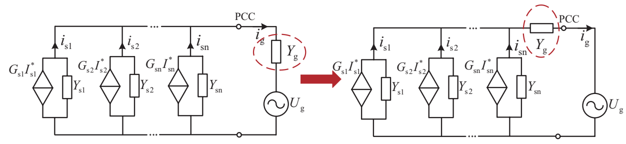

Fig. 5. Equivalent circuit diagram for multi-inverters paralleled system.

B. The Improved Minor Loop Gain Criterion

In aim to achieve precise attribution of responsibility to specific inverters causing system instability, the process of improving the loop gain criterion is mainly divided into two steps.

Firstly, equating the grid admittance with that of the grid-connected inverter's side to facilitate stability analysis for each inverter. Secondly, in this equivalence of grid admittance, utilizing the inverters' rated capacity as an allocation factor to accommodate their short-circuit ratio. The implementation steps are outlined as follows.

In the initial step, this paper relocated the grid admittance from the point of common coupling (PCC) to the inverter side. As shown in Fig. 5, the Kirchhoff's voltage and current laws (KVL and KCL) for the two circuits remain identical before and after the relocation. This indicates that the two circuits are equivalent.

Moreover, the parallel connection of admittances is equivalent to the sum of the individual admittances. Therefore, we modeled the original single grid admittance as n grid admittances connected in parallel. Subsequently, the grid admittance is allocated according to the principle of current allocation. The distribution ratio is proportional to the ratio of a specific inverter's output admittance to the total output admittance of all inverters, formulated as:

$$Y_{gi} = \left(Y_{si} / \sum_{i=1}^{n} Y_{si} \right) \bullet Y_g \tag{7}$$

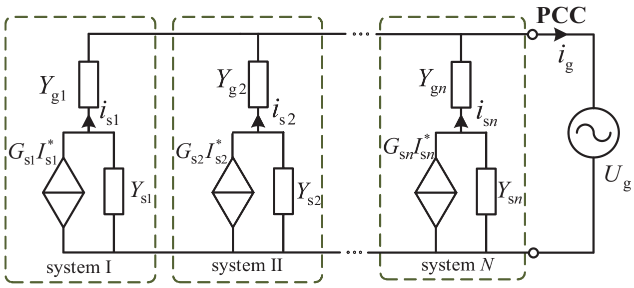

Fig. 6. Equivalent circuit diagram for IMLG.

The criterion can further be expressed as:

$$\frac{Y_{si}}{Y_{gi}} = \frac{Y_{si}}{\left(Y_{si} / \sum_{i=1}^{n} Y_{si}\right) \bullet Y_g} = Z_g \sum_{i=1}^{n} Y_{si} \tag{8}$$

This criterion is defined as the ratio of the output admittance of a single inverter to the equivalent grid admittance. An equivalent illustration is displayed in Fig. 6, where Y_{gi} represents the equivalent grid impedance of the i-th inverter.

It should be pointed out that the line impedance of the connecting lines between inverters is not negligible in the multi-inverter system. In this paper, the line impedance is merged with the grid-side inductance and resistance of the inverters. Compared to systems with long transmission lines, such as multi-wind farms, the line impedance between the inverters has much smaller values [25]. Therefore this equivalent approach is reasonable in reducing the difficulty of analysis while retaining the actual operating characteristics of the multi-inverter system.

At this point, this criterion allocates the equivalent grid admittance based solely on the inverter's output admittance, which inherently aligns it with the GMLG criterion and imposes certain constraints on stability analysis. Studies indicate that the capacity of the inverter significantly influences system stability. Especially, under constant conditions, higher output power from the inverter increases the risk of system instability [30]. Therefore, this paper incorporates the capacity factor when assigning the grid admittance, formulated as:

$$\tilde{Y}_{gi} = \left(S_{Bi}^{-1} Y_{si} / \sum_{i=1}^{n} S_{Bi}^{-1} Y_{si}\right) \bullet Y_g \tag{9}$$

where S_{Bi} is the rated capacity of the i-th inverter.

Despite this enhancement, the structure and form of the proposed criterion still maintain consistency with the traditional GMLG criterion. This refinement allows for a more comprehensive and accurate evaluation of the circuit's performance, while preserving the familiarity and applicability of the established criterion. It can also be expressed as:

$$\tilde{Y}_{gi} = S_{Bi}^{-1} Y_g \bullet \frac{Y_{si}}{\sum_{i=1}^{n} S_{Bi}^{-1} Y_{si}} \tag{10}$$

TABLE I
THE DESCRIPTION OF IMLG

Criterion	Expression	Characteristic
IMLG	$\frac{Y_{si}}{\left(S_{Bi}^{-1} Y_{si} / \sum_{i=1}^{n} S_{Bi}^{-1} Y_{si}\right) \bullet Y_g}$	I. It is enabled to analyze the stability of an inverter in a multi -inverters paralleled system. II. The introduction of inverters' rated capacity can reflect the short circuit impedance ratio of the parallel system.

The short-circuit ratio (SCR) is a crucial metric used to characterize the grid strength in grid-connected inverter systems, defined as [31], [32]:

$$\mathrm{SCR} = S_{ac} / S_B = \frac{U_n^2}{Z_g} \bullet \frac{1}{S_B} = \frac{U_n^2 Y_g}{S_B} \tag{11}$$

where S_{ac} is the system's short-circuit capacity; S_B is the rated capacity of the inverter; Y_g is the equivalent admittance; U_n is the rated voltage of the bus.

Additionally, the partial product term $S_B^{-1} Y_g$ in (10) can be further transformed as:

$$S_B^{-1} Y_g = U_n^2 \bullet \frac{Y_g}{S_B} \bullet \frac{1}{U_n^2} = \frac{S_{ac}}{S_B} \bullet \frac{1}{U_n^2} = SCR \bullet \frac{1}{U_n^2} \tag{12}$$

Finally, the expression for the proposed improved criterion can be summarized as:

$$IMLG = \frac{Y_{si}}{\tilde{Y}_{gi}} = \frac{Y_{si}}{\left(S_{Bi}^{-1} Y_{si} / \sum_{i=1}^{n} S_{Bi}^{-1} Y_{si}\right) \bullet Y_g} \tag{13}$$

Given that the rated voltage U_n of the bus remains constant, this criterion provides a generalized reflection of the SCR for inverter equipment to a certain extent. It indicates that a lower SCR associated with an inverter corresponds to a smaller equivalent grid admittance allocated to it, thereby resulting in a larger equivalent impedance value, and vice versa.

In conclusion, the description of the IMLG criterion can be summarized in the Table I.

It is worth explaining that the impedance criterion proposed in this paper considers the rated power of the inverter as the algorithm target for two major reasons: Firstly, the capacity of the inverter is a factor that affects the stability of the system [30]. Other conditions being constant, the higher the inverter capacity, the more unstable the system is. In this paper, the rated capacity is used as a reference, i.e., the output of the equipment is 100% of the rated capacity. Therefore, if the inverter equipment is stable according to the proposed criterion, the inverter and system will also be stable when the actual output power of the equipment is less than the rated capacity. As a result, adopting the rated capacity as the basis for calculation better reflects the performance and characteristics

TABLE II
PARAMETERS OF VARIOUS KINDS OF INVERTERS

Parameters	Symbol	Inverters	
		I	II/III/IV
Direct current voltage	U_{dc}/V	720	720
Inverter side inductance	L_1/mH	3.5	3/3.2/3.5
Filter capacitor	C_1/μF	30	10/20/30
Filter capacitor parasitic resistance	R_{C1}/Ω	0.8	0.3
Grid-side inductance	L_2/mH	0.15	0.15/0.5/0.8
Grid impedance	L_g/mH, R_g/Ω	0.05, 0.1	0.1, 0.1
dq-axis current reference value	I_{gdr}, I_{gqr}/A	40, 0	43/54/64, 0
Phase-locked loop parameters	K_{ppll}, K_{ipll}	20, 80	5, 80
Current loop parameters	K_{pi}	1	1/0.8/1.2
	K_{ii}	1000	1000/1200/1500

of the inverter equipment.

Secondly, in the practical application of new energy generation equipment such as wind power and photovoltaic power generation, the actual output power is constantly fluctuating due to the influence of the external environment [33], [34]. Therefore, it is difficult to judge the stability of the system in real time by using the actual power as the basis of calculation.

In conclusion, the impedance criterion based on the rated capacity can better satisfy the requirements of the system design, ensure the compatibility between the equipment and the system stability. Therefore, this paper takes the inverter's rated capacity as the calculation basis for the IMLG criterion.

Additionally, the proposed method can be used for stability analysis when real power is adopted. In this paper, we target the algorithm using the rated capacity, where the actual output is considered to be 100% of the rated capacity. This essentially represents a scenario where the actual value is used. Hence, the stability analysis can be carried out using this method when the actual output is known. The corresponding analyses and validations can be accessed in Appendix C.

III. COMPARISON OF LOOP GAIN STABILITY CRITERIA

Combining the theoretical analyses mentioned above, this paper compares and researches the characteristics of the MLG, GMLG and IMLG criterion under multi-inverters paralleled system with the identical and varying parameters.

A. The Multi-Inverters Grid-Connected System With Same Parameters

Table II lists the parameters for inverters I, II, III and IV. It needs to be clarified that that each inverter is stable when operated individually on the grid. By changing the number of I-type inverter at the PCC point and evaluating the stability of the parallel system, the Nyquist diagrams for the three stability

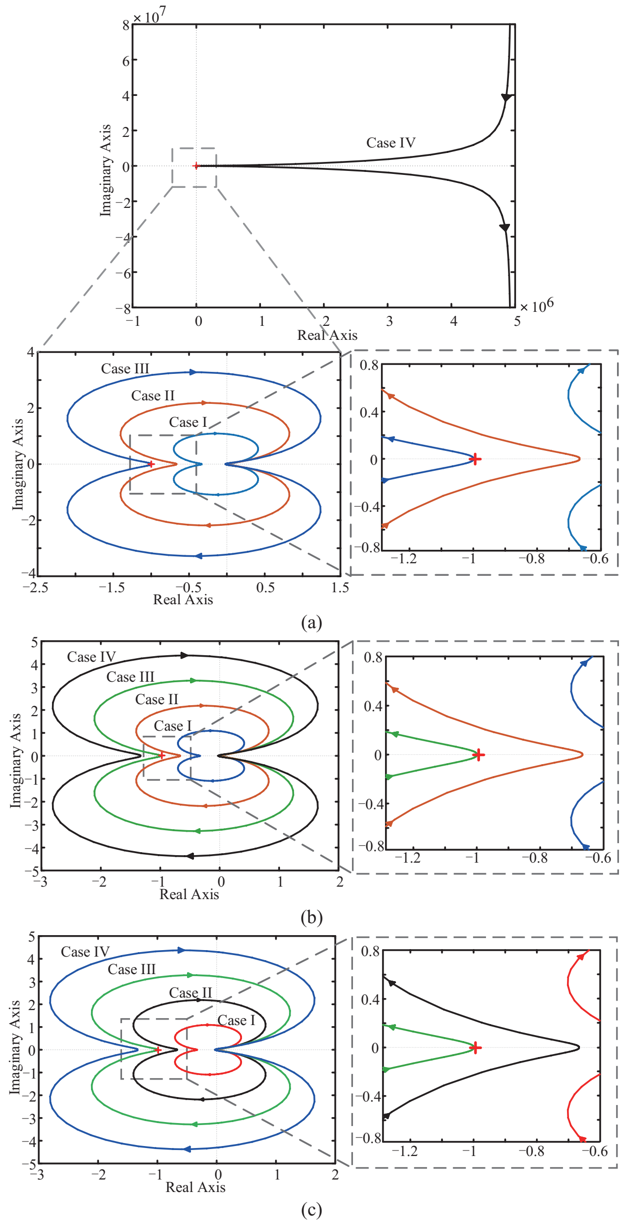

Fig. 7. The Nyquist diagrams for different stability criterion. (a) MLG, (b) GMLG and (c) IMLG.

criterions are presented in Fig. 7.

To portray the number of inverters in the grid-connected system, a single inverter is defined as case I, increasing unit by unit up to case IV. It should be mentioned that since the parameters of each inverter are identical, the stability of each inverter is the same, i.e., the Nyquist diagrams of each inverter plotted under the MLG and IMLG criterion overlap. If the Nyquist diagrams drawn by the criterion encloses the point (−1, *j*0), the inverters and the system are destabilized; otherwise, they are stable.

Based on Fig. 7(a), it is evident that when the inverters have identical parameters, increasing the number of inverters in the system from case II to case III shifts the system from stable to unstable. Moreover, increasing the number of parallel-connected inverters to case IV results in an infinitely large, unclosed curve in the Nyquist diagram according to the MLG criterion, which makes it hard to discern the stability of the multi-inverters paralleled system. Consequently, the MLG criterion is unsuitable for stability analysis in systems with a large number of grid-connected inverters.

Fig. 7(b) and (c) displays the Nyquist diagrams for the GMLG and IMLG criteria, respectively. The analyses from these two criteria are consistent, showing that the system becomes unstable when case III or more inverters are connected to the grid. In comparison, both the GMLG and IMLG criterion effectively support stability analysis for systems with a larger number of parallel-connected inverters.

B. The Multi-Inverters Grid-Connected System With Different Rated Capacity Parameters

In this subsection, the three stability criteria are further compared and analyzed by varying only the rated capacity of inverter I while keeping all other parameters unchanged as listed in Table II. The rated powers of inverters I-A, I-B, I-C, and I-D are set to 20, 25, 30 and 35 kW, respectively. Fig. 8 displays the Nyquist diagrams for the three stability criteria.

Fig. 8(a) describes the Nyquist diagrams plotted using the MLG criterion, indicating that all inverters are unstable with highly similar or indistinguishable graphs. Similar to with identical parameters, the MLG diagram becomes an unclosed curve extending to infinity when the number of inverters increases to four or more.

Based on the GMLG criterion, Fig. 8(b) indicates instability in the grid-connected system. However, this diagram represents the overall stability characteristics of the system without clearly delineating the stability of individual inverters within it.

The Nyquist diagram based on the IMLG criterion is illustrated in Fig. 8(c), depicts the Nyquist diagrams based on the IMLG criterion, revealing that inverters I-A and I-B are stable, whereas inverters I-C and I-D are unstable. This judgement is different from the MLG criterion and needs further experimental verification.

C. The Multi-Inverters Grid-Connected System With Different Parameters

To further compare the traditional criterion with the improved criterion, the stability of the system is evaluated with the inverters II, III, IV given in Table II to form the multi-inverters paralleled system with different parameters. Fig. 9 presents the Nyquist diagrams for the MLG, GMLG and IMLG criterions.

The diagram plotted by the MLG criterion is shown in Fig. 9(a), indicating that all three types of inverters are in a stable state. According to the GMLG criterion (see Fig 9(b)), the overall system is also stable. However, GMLG can only assess the stability of the entire grid-connected system and cannot analyze the operation of individual inverters. Fig. 9(c) displays the Nyquist diagram of the system based on the IMLG criterion.

It is evident that the improved IMLG criterion can identify the

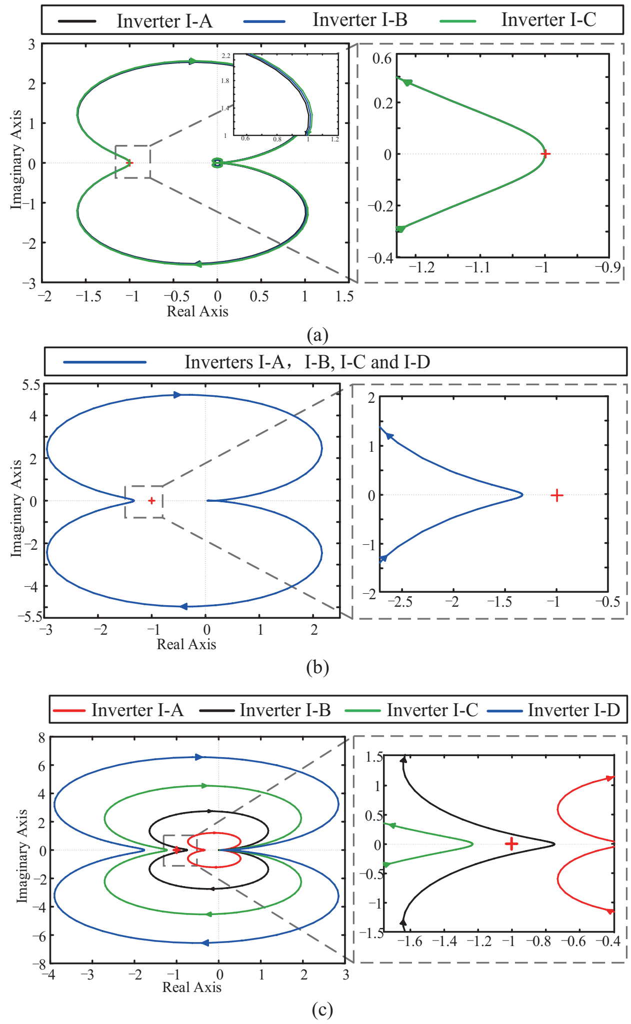

Fig. 8. The Nyquist diagrams for different stability criterion. (a) MLG, (b) GMLG and (c) IMLG.

operation status of each inverter within the system and accurately detect those that are unstable. According to IMLG, the inverter II in the parallel system operates stably, whereas inverters III and IV exhibit instability. This finding diverges from the assessments made by MLG and GMLG, highlighting the need for further experimental validation to confirm its accuracy.

IV. Example Verification

In this section, the experimental verification of the theoretical stability analyses for the three parallel systems mentioned above is presented. Additionally, further research was conducted on the practical application of the IMLG criterion.

A. Verification of the IMLG Criterion Validity

To verify the correctness of the theoretical analysis and the effectiveness of the proposed improved stability criterion, this paper conducts experimental tests with multi-inverters paralleled system. This experimental verification is carried out

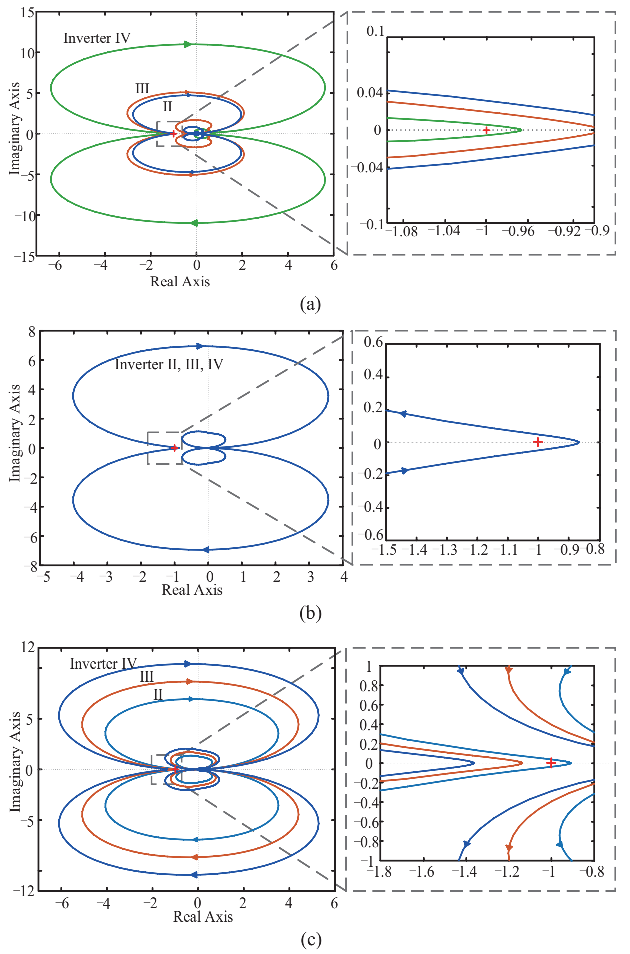

Fig. 9. The Nyquist diagrams for different stability criterion. (a) MLG, (b) GMLG and (c) IMLG.

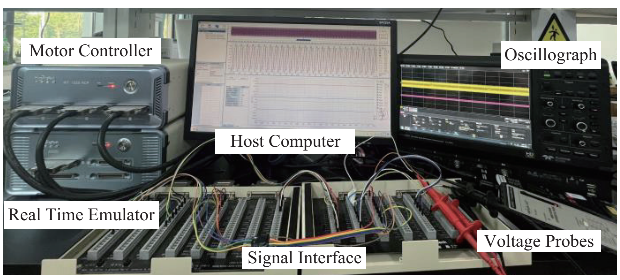

Fig. 10. Hardware-in-the-loop experimental platform.

through the hardware-in-the-loop test (HIL) platform, and the HIL platform is presented in Fig. 10.

Fig. 11 illustrates the experimental waveforms of the grid-connected system, depicting the grid-connected voltage and grid-connected current of cases I, II, and III.

Fig. 11(a) describes the experimental results of increasing the number of grid-connected inverter, i.e., the operating state transforms from case I to case II. It can be seen that when the number of parallel inverters increases to case II, the system remains stable. In Fig. 11(b), when the number of inverters increases from case II to case III, the system transitions from stable

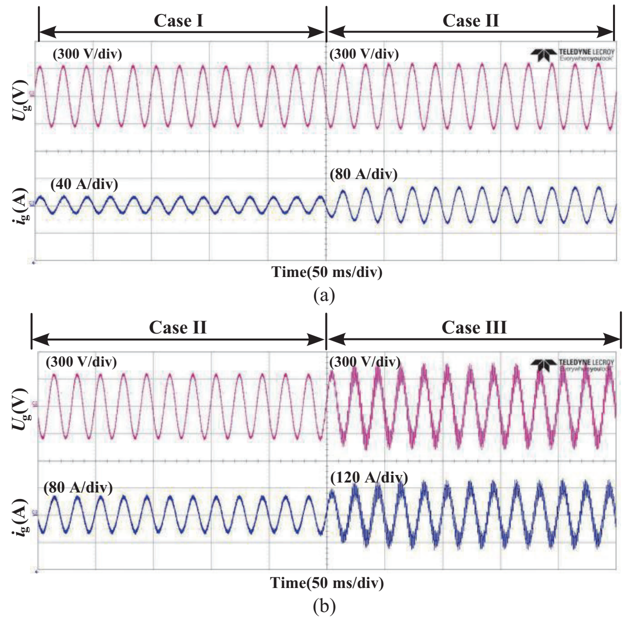

Fig. 11. Experimental waveforms for the multi-inverters grid-connected system with same parameters. Operation status changed from (a) case I to case II and (b) case II to case III.

to unstable. This is consistent with the analysis results in Section III. The experimental results indicate that the improved IMLG criterion can effectively determine the stability performance of multi-inverters paralleled system with identical parameters.

Fig. 12(a) presents experimental waveforms of the grid-connected voltage, grid-connected current, and active power during continuous operation of the inverters. From the results in Fig. 12(a), it is evident that the introduction of inverters I-C and I-D into the grid-connected system transitions the overall system from stability to instability. Fig. 12(b) displays waveforms of the grid-side currents of four inverters (I-A, I-B, I-C, and I-D) with varying rated power parameters sequentially connected to the grid. According to Fig. 12(b), it can be concluded that inverters I-A and I-B maintain stability while inverters I-C and I-D exhibit instability under continuous operation. This experimental outcome aligns with the stability analysis results using the IMLG criterion in Part B of Section III.

Fig. 13(a) illustrates the waveforms of grid-connected voltage, grid-connected current, and active power for inverters II, III, and IV when sequentially connected to the grid. Based on these experimental results, the system remains stable when only inverter II is connected, but becomes increasingly unstable as inverters III and IV are added to the grid, causing deviations in active power from the commanded value.

Fig. 13(b) describes the grid-side current waveforms of inverters II, III, and IV in the parallel system. According to the control results shown in Fig. 13(b), inverter II operates stably in the parallel configuration, whereas inverters III and IV exhibit instability, leading to overall instability of the parallel system. This observation is consistent with the judgment of the IMLG criterion in Section III, Part C.

From the above analysis, it can be concluded that, unlike the MLG and GMLG criteria, the stability analysis based

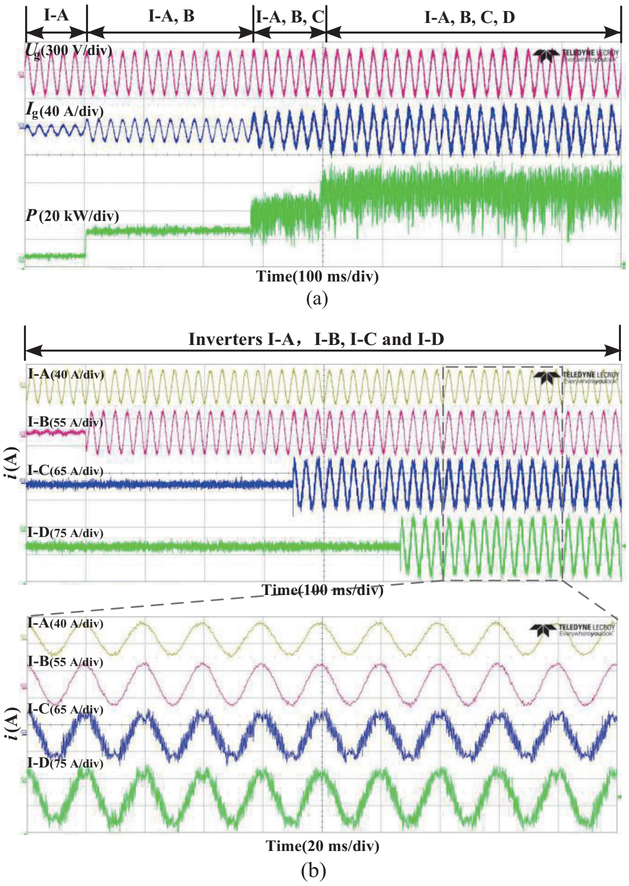

Fig. 12. Experimental waveforms for the multi-inverters grid-connected system with different rated capacity parameters. (a) Multi-inverters paralleled system with different rated capacity parameters. (b) The operation status of inverter I- A, I- B, I- C and I- D.

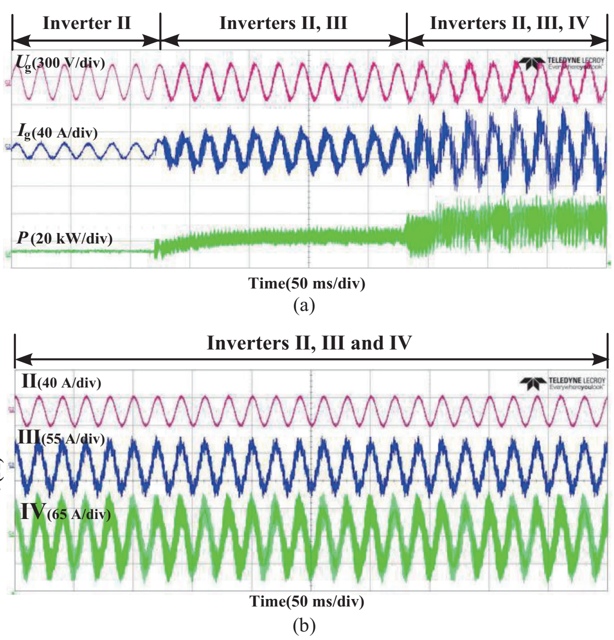

Fig. 13. Experimental waveforms for the multi-inverters grid-connected system with different parameters. (a) Multi-inverters paralleled system with different parameters. (b) The operation status of inverters II, III, and IV.

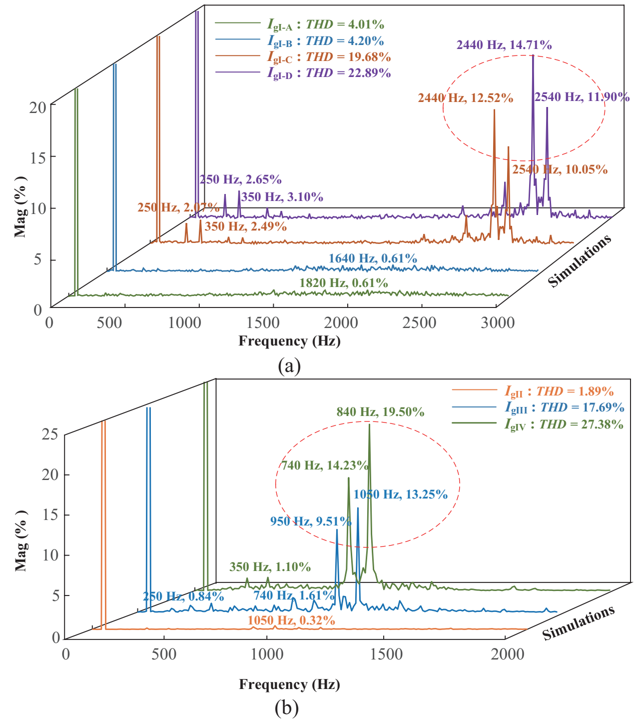

Fig. 14. FFT resonance analysis of parallel systems. (a) FFT analysis results of multi-inverter grid-connected systems with different rated capacity parameters. (b) FFT analysis results of multi-inverter grid-connected systems with different parameters.

on improved IMLG criterion aligns with the experimental verification results and it can accurately identify the inverters that cause system instability.

The experimental waveforms presented in Figs. 12 and 13 exhibit some irregular burrs. When outputting the experimental results, some burrs and stray waves will inevitably be generated due to poor contact of the measurement probe. This may be one of the reasons for irregular burrs in the waveforms. To investigate the underlying reason for the generation of these waveform anomalies, this study conducted fast Fourier transform (FFT) analysis of the multi-inverter parallel system. Specifically, the analysis was performed under two conditions: 1) by varying the rated capacity of the inverters, and 2) by considering the multi-inverter parallel system with different system parameters.

The results of the grid-connected current analysis for each inverter are illustrated in Fig. 14. From the results of the FFT analysis, it is evident that there are a substantial number of medium- and high-frequency resonances in addition to low-frequency oscillation in the grid-connected currents of each inverter. It is the main reason for the irregular burrs in the experimental waveforms.

In conclusion, the comparative analysis of different loop gains stability criterions are summarized in Table III.

B. IMLG-Based Analysis of the Effect of Inverters Parameters on the Stability of Parallel System

To further probe the application value of the proposed

TABLE III
COMPARATIVE ANALYSIS OF DIFFERENT LOOP GAINS STABILITY CRITERIA

Stability criterion	Expression	Specificities
MLG	$Y_{si} / \left(Y_g + \sum_{j=1, j\neq i}^{n} Y_{sj} \right)$	I. The stability of each inverter can be determined. II. For grid-connected systems with a large number of inverters connected, this criterion is no longer applicable.
GMLG	$Z_g \sum_{i=1}^{n} Y_{si}$	I. It is capable to judge the overall operational status of the system. II. In the case of instability, it is not possible to determine the dominant inverter causing the system instability.
IMLG	$\dfrac{Y_{si}}{\left(S_{Bi}^{-1} Y_{si} / \sum_{i=1}^{n} S_{Bi}^{-1} Y_{si} \right) \cdot Y_g}$	I. It correctly judge the stability of grid-connected inverters. II. It can determine the responsibility of unstable inverters. III. Accurate stability analysis of multi-inverters paralleled system with different parameters.

method, this paper analyzed the effect of inverters parameters on system stability based on the IMLG criterion.

This paper constructed the parallel system of three inverters utilizing the I-type inverters in the parameters of Table II, and analyzed the effects of the inverter parameters on the stability of the parallel system by varying the inverter-side inductance L_1, the grid-side inductance L_2, the filter capacitance C_1 and the grid inductance L_g, respectively. And the stability analysis of the parallel system under each case by IMLG criterion is depicted in Fig. 15.

It is worth mentioning that the Nyquist diagrams presented as red lines are all unaltered initial data, which can be regarded as a set of reference data.

Fig. 15(a) displays the stability results of the parallel system with L_1 at 0.5, 3.5, and 10 mH, respectively. It can be intuitively observed that as the value of inverter side inductance increases, the system gradually transforms from instability to stability with a large stability margin according to the judgement of the proposed criterion. Based on Fig. 15(b), it can be concluded that as the value of L_2 gradually increases from 0.05, 0.15, 0.3 mH, the parallel system gradually varies from stable state to instability. On the other hand, compared to L_1, L_2 has a greater impact on the system stability, and a smaller value can alter its stability.

Fig. 15(c) depicts the Nyquist plot of the parallel system when C_1 is gradually enlarged from 10, 30, 40 μF. Similar to L_1, the parallel system changes from instability to stability as C_1 increases. Moreover, the change in C_1 also has a significant influence on the stability of the system. Finally, the effect of L_g on stability is analyzed. According to the judgement of Fig. 15(d), the stability of the system deteriorates as L_g increases from 0.01, 0.35, 0.5 mH and finally instability.

Regarding its accuracy, this paper provides the corresponding experimental validation and detailed analyses of the grid-connected current, grid-connected voltage, and active power for various cases.

Fig. 16 illustrates the experimental waveforms of a grid-

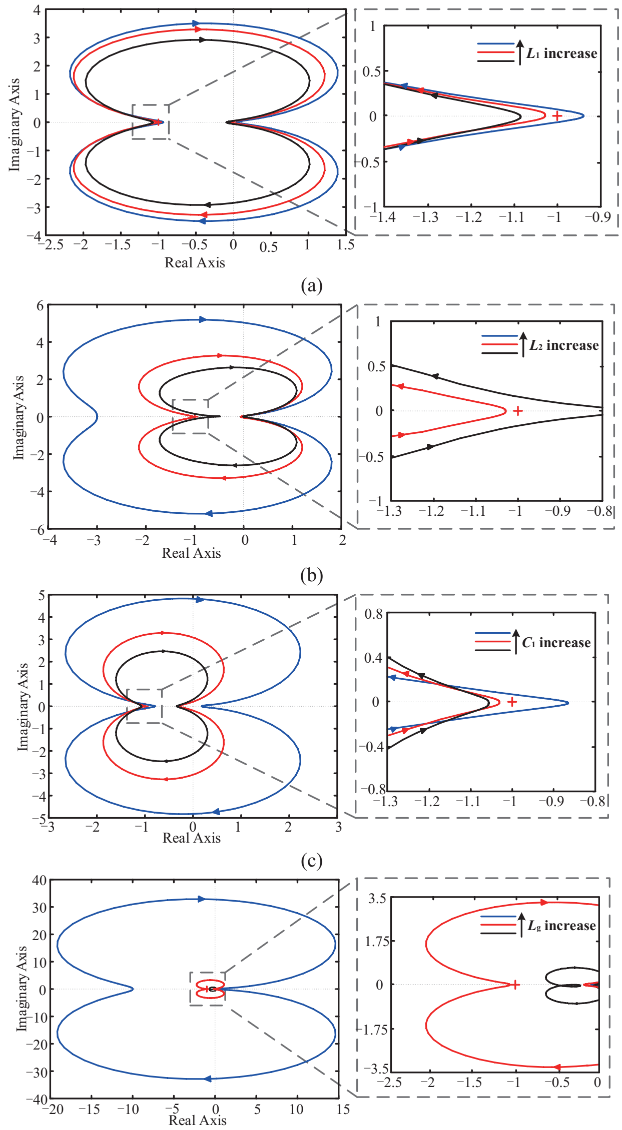

Fig. 15. Nyquist diagrams for different parameters based on the IMLG criterion. (a) Inverter side inductance L_1, (b) grid-side inductance L_2, (c) filter capacitor C_1 and (d) grid inductance L_g.

connected system consisting of three inverters of type I with initial parameters, i.e., the experimental results corresponding to the lines labelled in red in the Nyquist diagrams of the four cases in the previous description. It's simple to identify that the system is unstable in this case, and this matches the previous analysis.

Based on Fig. 17, it is clearly shown that the parallel system is unstable when L_1 is 0.5 mH and stable when L_1 is 10 mH. This is consistent with the results of the stability analysis in Fig. 15(a) and also proves again the validity of the IMLG criterion.

Fig. 18 illustrates the experimental waveforms of grid-connected current, voltage and active power for the parallel system when L_2 is 0.05 mH and 0.3 mH. When L_2 takes smaller values, the system is stable; while when L_2 increases, the system is instability. This result is identical to the judgement result in Fig. 15(b).

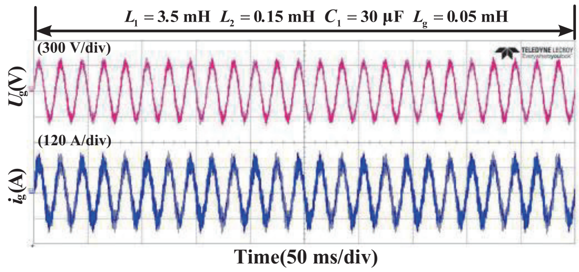

Fig. 16. Experimental results of parallel system consisting of I-type inverters.

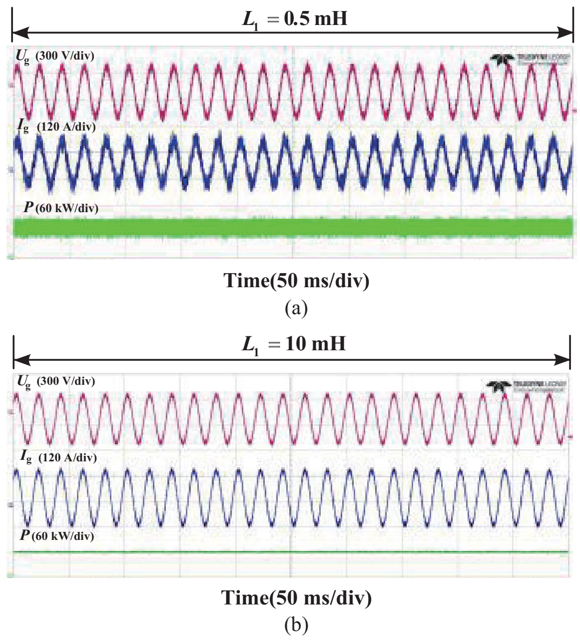

Fig. 17. Experimental results of parallel system with varying the inverter-side inductance L_1. (a) L_1 = 0.5 mH and (b) L_1 = 10 mH.

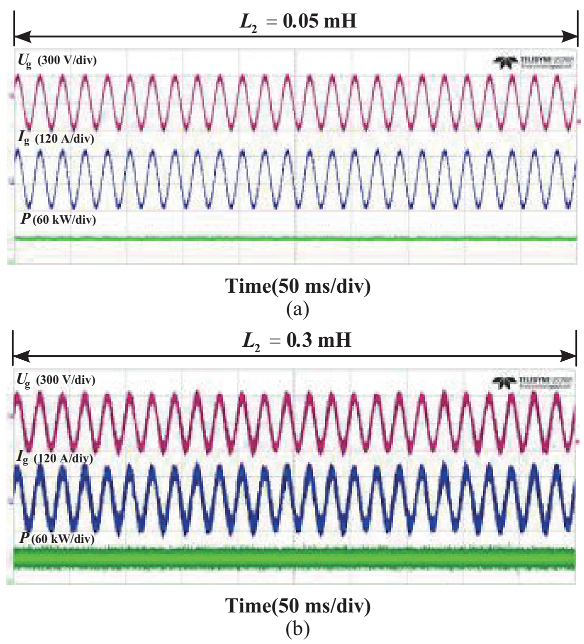

Fig. 18. Experimental results of parallel system with varying the grid-side inductance L_2. (a) L_2 = 0.05 mH and (b) L_2 = 0.3 mH.

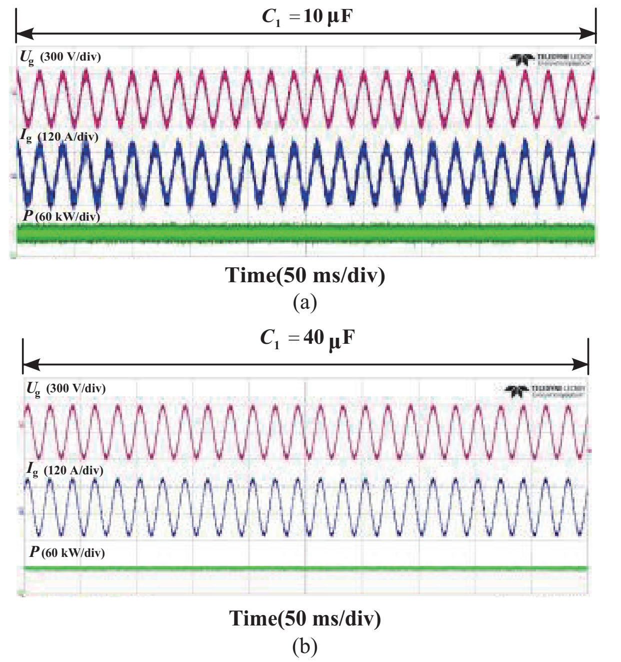

Fig. 19. Experimental results of parallel system with varying the filter capacitor C_1. (a) C_1 = 10 μF and (b) C_1 = 40 μF.

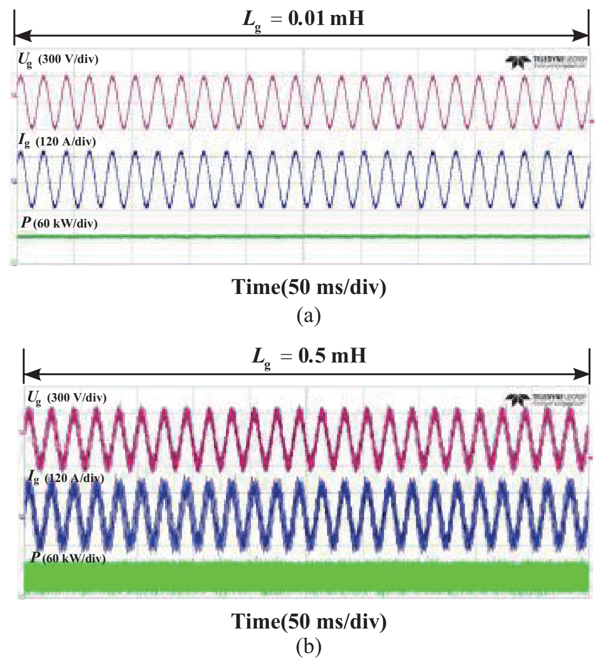

Fig. 20. Experimental results of parallel system with varying the grid inductance L_g. (a) L_g = 0.01 mH and (b) L_g = 0.5 mH.

In Fig. 19(a), where C_1 is 10 μF, the system fails to operate stably. Conversely, in Fig. 19(b), when C_1 is 40 μF, the system becomes stable. This observation is in alignment with the results of the stability analysis presented previously in Fig. 15(c).

Fig. 20 depicts the results of the experimental plots of the multi-inverters paralleled system at different L_g, respectively. Where the system is stable when L_g is 0.01 mH and unstable when L_g is 0.5 mH. The experimental results under this case also verify the validity and correctness of the proposed criterion.

Furthermore, based on the IMLG criterion is the feature that can correctly analyze the stability of individual inverters in the multi-inverters paralleled system. When instability or faults occur in the multi-inverters paralleled system, the MLG criterion cannot accurately determine the stability of the inverters due to the fact that it is unable to satisfy the stability analysis of the parallel system with an excessive number of inverters. The GMLG criterion can only evaluate the overall operation of the system, therefore the GMLG criterion is also unable to identify the inverters that cause the system instability. In contrast, the utilization of the IMLG criterion can accurately locate and evaluate one or more unstable inverters in the multi-inverters paralleled system. Therefore, the stability of the parallel system can be restored by adjusting the parameters of the unstable inverters, etc., guided by the stability analysis results of the IMLG criterion. It can be concluded that the proposed method has practical value for the stable operation of actual systems.

V. Conclusions

This paper focuses on the LCL-type inverter and their associated systems, proposing the IMLG that considers the equipment capacity. By constructing a complete frequency domain admittance model for the multi-inverters paralleled system, this criterion adequately accounts for the impact of inverter's capacity and short-circuit ratio on system stability. The main conclusions are as follows:

1) The proposed improved IMLG can be summarized as follows: the grid impedance is equated to the inverter side, taking into account the inverter's rated capacity. This allows it to reflect, to some extent, the short-circuit impedance ratio of the inverter. It comes out that a higher short-circuit impedance ratio corresponds to a larger equivalent grid admittance allocated to the inverter, resulting in a smaller equivalent impedance value and a more stable system.
2) A comparison between the traditional MLG, GMLG criteria and the improved IMLG criterion reveals that as the number of paralleled inverters increases, the Nyquist curve generated by the MLG criterion becomes an infinitely unclosed curve, rendering it unsuitable for stability analysis of multi-inverters paralleled system. The GMLG criterion can only analyze the entire inverter system, unable to determine the operating condition of each inverter. When the system becomes unstable, it cannot accurately identify the unstable inverters. In contrast, the IMLG criterion can accurately analyze the stability of multi-inverters system with both identical and varying parameters. It is furthermore capable of correctly determining the operating status of each inverter in a grid-connected system and precisely identifying the specific inverter that is causing the instability.
3) The improved loop gain criterion proposed in this paper is aimed at analyzing and researching the same type of grid-connected inverters under changing parameter conditions. At present, the new power supply system is gradually presenting the characteristic of heterogeneous inverters paralleled system (HIPS), and it is presented in the form of coexistence of two types of inverters, i.e., grid-following inverters (GFL) and grid-forming inverters (GFM), therefore, it is worthwhile to further investigate the stability analysis of the grid-connected system constituted by different types of inverters. Additionally, most of the existing stability researches are based on white box systems, while there are still many gaps in the stability analyses of black/grey box systems where the internal structure and parameters are not known [35]. From the expression of the IMLG criterion, among the electrical quantities required for stability analysis, the output conductance and grid conductance of the inverter can generally be measured by field instruments, while the rated capacity of the inverter can be easily obtained from its nameplate, thus little a priori knowledge is required. Therefore, the criterion might have some application to black/grey box systems, which is worth further investigation.

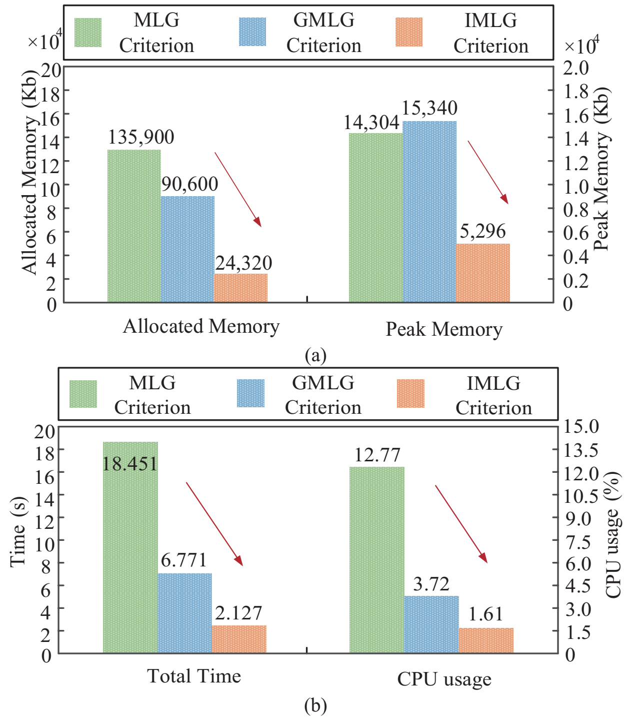

Fig. 21. Statistical results on computational efficiency of MLG, GMLG and IMLG criterion. (a) Allocated memory and peak memory. (b) Total time and CPU usage.

Appendix

A. Comparative Analysis of Stability Criteria for Different Loop Gains

This paper uses Profile function in MATLAB/Simulink to compare the computational memory consumption and CPU usage of the MLG, GMLG, and improved criterion IMLG, as shown in the Fig. 21.

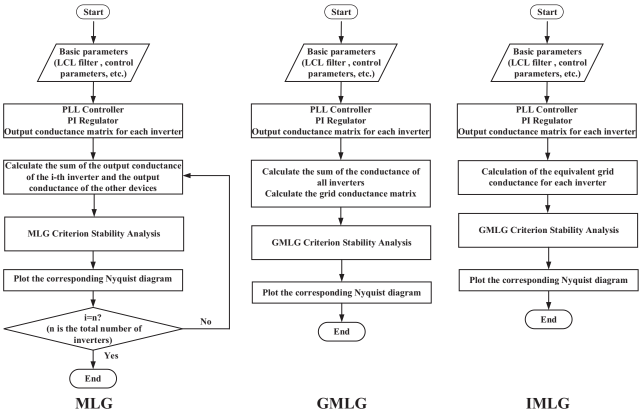

Fig. 22. Flowchart for each criterion.

It is worth mentioning that all comparisons of computational resources are analyzed for procedures of multi-inverters paralleled system with different parameters. Except for the difference in the analysis method of the criterion itself, the number of inverters, parameters, modelling approach, etc. are identical. Moreover, all three procedures are invoked only once, and the case where the value of the operation is stored in the workspace after multiple invocations does not occur.

The proposed criterion IMLG occupies 24320 kB of running memory, with a peak memory usage of 5296 kB. It completes execution in 2.127 s with a CPU usage of 1.61%. A comparison reveals that the IMLG criterion's runtime is 11.5% shorter than that of the MLG criterion, and the CPU usage is 12.6% lower than that of the GMLG criterion, demonstrating the significant computational efficiency of the improved criterion.

The better computational efficiency of the proposed criterion can be illustrated more intuitively in the Fig. 22.

The proposed IMLG criterion treats each inverter as a separate subsystem through equivalent grid conductance. Although it is also required to analyze each inverter, there is no duplication of computation in the analysis of IMLG compared to MLG. As a result, it uses significantly less memory and computation time. In addition, unlike the GMLG criterion, IMLG need not calculate all the data simultaneously. Therefore, the peak memory is also minimum.

B. Influence of Inverter Capacity on System Stability

To better illustrate the effect of inverter capacity on system stability, this paper uses the parameters of inverter II in Section III and conduct simulations where only the inverter's capacity is varied. The simulation results of the grid-connected current and voltage, active and reactive power before and after the capacity change are presented in Fig. 23.

According to Fig. 23, it can be concluded that the stability of the grid-connected system transforms from stable to unstable after the inverter's capacity has been increased by 30 kW. This again proves that the inverter capacity has an effect on the system stability.

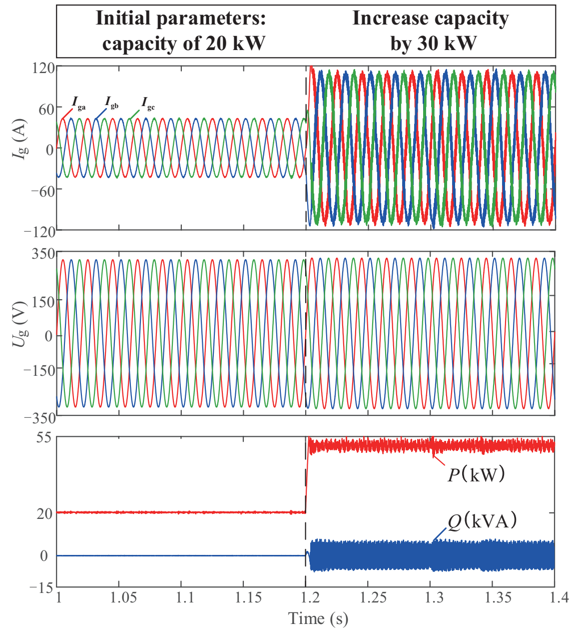

Fig. 23. Simulation results of varying inverter's capacity.

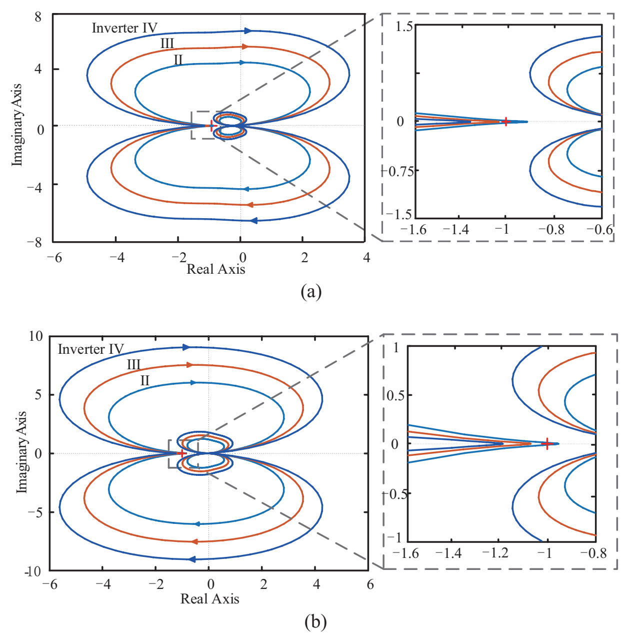

Fig. 24. The Nyquist diagrams for IMLG. (a) Inverters' output at 50% of rated capacity. (b) Inverters' output at 90% of rated capacity.

C Stability Analysis Utilizing the Actual Power

Inverter types II, III and IV are still taken as the research objects to construct the multi-inverters parallel system with different parameters. Stability analysis and simulation verification are performed when the output is 50% and 90% of the rated capacity, respectively. The Nyquist diagram plotted by the proposed criterion when different actual output powers are employed as the algorithm's objective is depicted in Fig. 24.

Based on Fig. 24, it could be observed that whether the output power is 50% or 90% of the rated capacity, the Nyquist

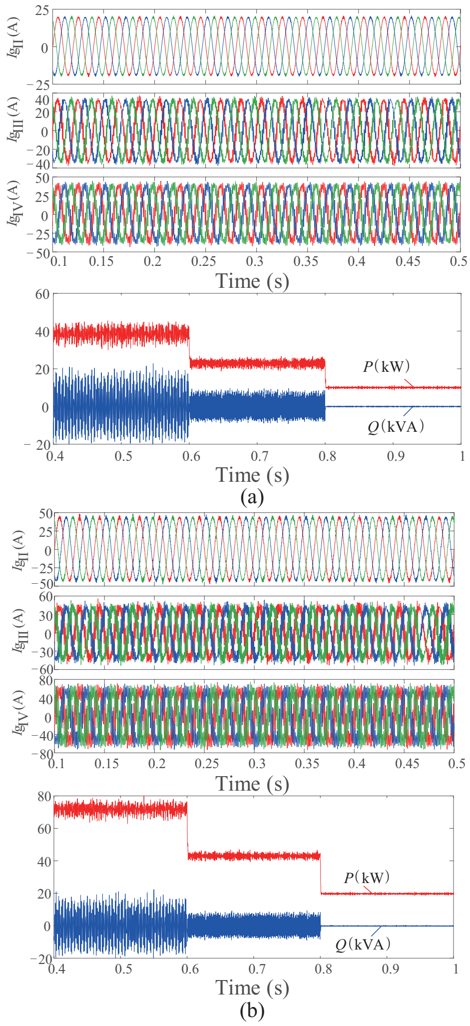

Fig. 25. Simulation results of grid-connected currents of inverters II, III, IV and active and reactive power of the parallel system. (a) Inverters' output at 50% of rated capacity. (b) Inverters' output at 90% of rated capacity.

diagram of inverter II is not enclosing the point $(-1, j0)$, while the Nyquist diagrams of both inverters III and IV are enclosing the point $(-1, j0)$. It implies that under the judgement of the proposed criterion, inverter II is stable and inverters III and IV are unstable. This paper verified the results of this stability analysis by simulation experiments.

The simulation experiments firstly analyzed the grid-connected currents of each inverter in the parallel system as shown in Fig. 25. At the actual output of 50% and 90% of the rated capacity, inverter II is still operating stable, while inverters III and IV are unstable. After running the experiment for 0.6 s and 0.8 s, inverters IV and III were sequentially removed from the parallel system. It was observed that the active power output of the parallel system gradually transitioned from instability to stability.

This experimental result was consistent with the aforementioned stability analysis, and it also proved that the proposed method can accurately analyze the stability of the parallel system when the actual values are known. This also implies that the IMLG criterion serves both as a sufficient condition and a necessary condition.

References

[1] S. He, D. Zhou, X. Wang, and F. Blaabjerg, "Passivity-based multisampled converter-side current control of LCL-filtered VSCs," in *IEEE Transactions on Power Electronics*, vol. 37, no. 11, pp. 13848–13860, Nov. 2022.

[2] T. Fang, S. Shen, Y. Jin, and X. Ruan, "Robustness investigation of multi-inverter paralleled grid-connected system with LCL-filter based on the grid-impedance allocation mechanism," in *IEEE Transactions on Power Electronics*, vol. 36, no. 12, pp. 14508–4524, Dec. 2021.

[3] T. Roinila and T. Messo, "Online grid-impedance measurement using ternary-sequence injection," in *IEEE Transactions on Industry Applications*, vol. 54, no. 5, pp. 5097–5103, Sept.-Oct. 2018.

[4] C. Y. Tang and J. H. Jheng, "An active power ripple mitigation strategy for three-phase grid-tied inverters under unbalanced grid voltages," in *IEEE Transactions on Power Electronics*, vol. 38, no. 1, pp. 27–33, Jan. 2023.

[5] Y. Chen, A. Sangwongwanich, M. Huang, S. Pan, X. Zha, and H. Wang., "Failure risk assessment of grid-connected inverter with parametric uncertainty in LCL filter," in *IEEE Transactions on Power Electronics*, vol. 38, no. 8, pp. 9514–9525, Aug. 2023.

[6] M. Lu, X. Wang, P. C. Loh, and F. Blaabjerg, "Resonance interaction of multi-parallel grid-connected inverters with LCL filter," in *IEEE Transactions on Power Electronics*, vol. 32, no. 2, pp. 894–899, Feb. 2017.

[7] X. Wang and F. Blaabjerg, "Harmonic stability in power electronic-based power systems: concept, modeling, and analysis," in *IEEE Transactions on Smart Grid*, vol. 10, no. 3, pp. 2858–2870, May 2019.

[8] Q. Fu, W. Du, and H. Wang, "Analysis of harmonic oscillations caused by grid-connected VSCs," in *IEEE Transactions on Power Delivery*, vol. 36, no. 2, pp. 1202–1210, Apr. 2021.

[9] J. Sun, G. Wang, X. Du, and H. Wang, "A theory for harmonics created by resonance in converter-grid systems," in *IEEE Transactions on Power Electronics*, vol. 34, no. 4, pp. 3025–3029, Apr. 2019.

[10] M. Lu, "An inrush current limiting strategy for virtual-oscillator-controlled grid-forming inverters," in *IEEE Transactions on Power Electronics*., vol. 38, no. 3, pp. 1501–1510, Sept. 2023.

[11] C. Xie, K. Li, J. Zou, D. Liu, and J. M. Guerrero, "Passivity-based design of grid-side current-controlled LCL -type grid-connected inverters," in *IEEE Transactions on Power Electronics*, vol. 35, no. 9, pp. 9813–9823, Sept. 2020.

[12] D. Yang and X. Wang, "Unified modular state-space modeling of grid-connected voltage-source converters," in *IEEE Transactions on Power Electronics*, vol. 35, no. 9, pp. 9700–9715, Sept. 2020.

[13] C. Li, J. Liang, L. M. Cipcigan, W. Ming, F. Colas, and X. Guillaud, "DQ impedance stability analysis for the power-controlled grid-connected inverter," in *IEEE Transactions on Energy Conversion*, vol. 35, no. 4, pp. 1762–1771, Dec. 2020.

[14] J. Khazaei, Z. Tu, A. Asrari, and W. Liu, "Feedback linearization control of converters with LCL filter for weak AC grid integration," in *IEEE Transactions on Power Systems*, vol. 36, no. 4, pp. 3740–3750, Jul. 2021.

[15] H. Li, W. Wu, M. Huang *et al.*, M. Liserre, and F. Blaabjerg, "Design of PWM-SMC controller using linearized model for grid-connected inverter with LCL filter," in *IEEE Transactions on Power Electronics*, vol. 35, no. 12, pp. 12773–12786, Dec. 2020.

[16] J. Lin, M. Su, Y. Sun, D. Yang, S. Xie, W. Xiong, and G. Zhang, "Frequency coupling suppression control strategy for single-phase grid-tied inverters in weak grid," in *IEEE Transactions on Industrial Electronics*, vol. 69, no. 9, pp. 8926–8938, Sept. 2022.

[17] Q. Qian, S. Xie, J. Xu, K. Xu, S. Bian, and N. Zhong, "Output impedance modeling of single-phase grid-tied inverters with capturing the frequency-coupling effect of PLL," in *IEEE Transactions on Power Electronics*, vol. 35, no. 5, pp. 5479–5495, May 2020.

[18] J. Sun, "Impedance-based stability criterion for grid-connected inverters," in *IEEE Transactions on Power Electronics*, vol. 26, no. 11, pp. 3075–3078, Nov. 2011.

[19] Xiaogang Feng, Jinjun Liu, and F. C. Lee, "Impedance specifications for stable DC distributed power systems," in *IEEE Transactions on Power Electronics*, vol. 17, no. 2, pp. 157–162, Mar. 2002.

[20] D. Dong, B. Wen, D. Boroyevich, P. Mattavelli, and Y. Xue, "Analysis of

phase-locked loop low-frequency stability in three-phase grid-connected power converters considering impedance interactions," in *IEEE Transactions on Power Electronics*, vol. 62, no. 1, pp. 310–321, Jan. 2015.

[21] B. Wen, D. Dong, D. Boroyevich, R. Burgos, P. Mattavelli, and Z. Shen, "Impedance-based analysis of grid-synchronization stability for three-phase paralleled converters," in *IEEE Transactions on Power Electronics*, vol. 31, no. 1, pp. 26–38, Jan. 2016.

[22] C. Zhang, M. Molinas, A. Rygg, and X. Cai, "Impedance-based analysis of interconnected power electronics systems: impedance network modeling and comparative studies of stability criteria," in *IEEE Journal of Emerging and Selected Topics in Power Electronics*, vol. 8, no. 3, pp. 2520–2533, Sept. 2020.

[23] X. Wang, F. Blaabjerg, M. Liserre, Z. Chen, J. He, and Y. Li, "An active damper for stabilizing power-electronics-based AC systems," in *IEEE Transactions on Power Electronics*, vol. 29, no. 7, pp. 3318–3329, Jul. 2014.

[24] Q. Ye, R. Mo, Y. Shi, and L. Hiu, "A unified Impedance-based stability criterion (UIBSC) for paralleled grid-tied inverters using global minor loop gain (GMLG)," in *Proceedings of ECCE*, Montreal, QC, Canada, 2015, pp. 5816–5821.

[25] X. Peng and H. Yang, "Stability analysis of multi-paralleled grid-connected inverters including distribution parameter characteristics of transmission lines," in *CSEE Journal of Power Energy Systems*, vol. 7, no. 1, pp. 93–104, Jan. 2021.

[26] Y. Han, M. Yang, H. Li, P. Yang, L. Xu, E. A. A. Coelho, and J. M. Guerrero, "Modeling and stability analysis of LCL-type grid-connected inverters: a comprehensive overview," in *IEEE Access*, vol. 7, pp. 114975–115001, 2019.

[27] T. Fang, S. Shen, Y. Jin *et al*., "Robustness investigation of multi-inverter paralleled grid-connected system with LCL-filter based on the grid-impedance allocation mechanism," in *IEEE Transactions on Power Electronics*, vol. 36, no. 12, pp. 14508–14524, Dec. 2021.

[28] R. Zhang, C. Zhang, X. Xing, S. Chi, C. Liu, and J. Fang, "Modeling and attenuation of common mode resonance current for improved LCL-type parallel inverters in PV plants" in *IEEE Transactions on Industrial Informatics*, vol. 20, no. 4, pp. 5193–5205, Apr. 2024.

[29] W. Cao, S. Wang, H. Kang, K. Liu, Q. Wang, and J. Zhao, "Inherent interaction analysis for harmonic oscillations in the multi-paralleled grid-connected inverter system using a sum type criterion: global admittance (GA)," in *IEEE Access.*, vol. 8, pp. 8275–8285, 2020.

[30] M. Yang, F. Liu, Y. Wang, and W. Cao, "Maximum capacity assessment for multi-paralleled grid-connected inverters using global-admittance based harmonic stability analysis," in *Proceedings of 2021 IEEE Sustainable Power and Energy Conference (iSPEC)*, Nanjing, China, 2021, pp. 2787–2792.

[31] H. Yuan, H. Xin, D. Wu, W. Wang, and Y. Zhou, "Small-signal stability assessment of multi- converter-based-renewable systems with STATCOMs based on generalized short-circuit ratio," in *IEEE Transactions on Energy Conversion*, vol. 37, no. 4, pp. 2889–2902, Dec. 2022.

[32] J. Z. Zhou, H. Ding, S. Fan, Y. Zhang and A. M. Gole, "Impact of short-circuit ratio and phase-locked-loop parameters on the small-signal behavior of a VSC-HVDC converter," in *IEEE Transactions on Power Delivery*, vol. 29, no. 5, pp. 2287–2296, Oct. 2014,

[33] M. Shafiullah, S. D. Ahmed and F. A. Al-Sulaiman, "Grid integration challenges and solution strategies for solar PV systems: a review," in *IEEE Access*, vol. 10, pp. 52233–52257, 2022.

[34] J. Zhang, N. Zhang, and Y. Ge, "Energy storage placements for renewable energy fluctuations: a practical study," in *IEEE Transactions on Power Systems*, vol. 38, no. 5, pp. 4916–4927, Sept. 2023.

[35] Y. Zhu, Y. Gu, Y. Li, and T. C. Green, "Participation analysis in impedance models: the grey-box approach for power system stability," in *IEEE Transactions on Power Systems*, vol. 37, no. 1, pp. 343–353, Jan. 2022.

Yuhan Duan received the B.S. degree from Qingdao University of Science and Technology, Qingdao, China in 2023. She is currently pursuing a master's degree with the College of New Energy, China University of Petroleum (East China), Qingdao, China. Her current research interests include modeling, control and stability analysis of grid-connected inverters.

Pingjuan Ge received the B.S. and Ph.D. degrees both in electrical engineering from Anhui University, Hefei, China, and Hunan University, Changsha, China, in 2017 and 2022, respectively. She is currently working as a Lecture with the New Energy College, China University of Petroleum (East China), Qingdao, China. Her current research interests include modeling and transient stability analysis of the power-electronic- based power systems.

Hailiang Xu received the B.S. and Ph.D. degrees both in electrical engineering from China University of Petroleum (East China), Qingdao, China, and Zhejiang University, Hangzhou, China, in 2008 and 2014, respectively. He is currently working as a Professor with the New Energy College, China University of Petroleum (East China), Qingdao, China. His current research interests include renewable energy generation and microgrid.

Hongbin Lin received the B.S. and M.S. degrees from the China University of Petroleum (East China), Qingdao, China, in 2021 and 2024, respectively. He is currently working toward the Ph.D. degree in the Key Laboratory of Control of Power Transmission and Conversion, Ministry of Education, Shanghai Jiao Tong University, Shanghai, China. His current research interests include modeling and stability analysis of the multi-inverter paralleled system.